Journal of Spectroscopy and Molecular Sciences

Journal Homepage: https://dergipark.org.tr/tr/pub/jsms

Vibrational (FT-IR and FT-Raman), NMR and quantum chemical investigations on 7-Methylcoumarin

Yusuf Erdogdu[1,*], Ömer Dereli[2], Ebru Karakaş Sarıkaya[2]

[1]Department of Physics, Faculty of Science, Gazi University, Ankara, Turkey
[2]Department of Physics, Faculty of A. K. Education, Konya Necmettin Erbakan University, Konya, Turkey

*Correspondence: yerdogdu@gazi.edu.tr (Yusuf Erdogdu)
ORCIDs Yusuf Erdogdu: https://orcid.org/0000-0001-7695-3834
Omer Dereli: https://orcid.org/ 0000-0002-9031-8092
Ebru Karakaş Sarıkaya: https://orcid.org/0000-0003-2149-9341

Abstract: In this article, the vibrational spectra of 7-Methylcoumarin were reported and discussed. The Infrared and Raman spectra of 7-Methylcoumarin in solid state were recorded in the region 4000-400 cm-1 and 3500-50 cm-1, respectively. The ground state spectroscopic and structural data of 7-Methylcoumarin were calculated utilizing Density Functional Theory (DFT) employing B3LYP functional that contains 6-311++G(d,p) and cc-pVDZ basis sets. After than the geometry optimization was performed, the vibrational frequencies were calculated. Furthermore, the total energy distribution (TED) of the vibration mode was determined based on the fundamental vibrational modes. These calculations were performed with PQS program using scaled quantum mechanics (SQM) method.

Keywords: 7-Methylcoumarin; DFT; FT-IR; FT-Raman; Molecular Structure; Vibrational spectra.

1. Introduction

"Coumarin has the characteristic odour like that of vanilla beans. It is used for the preparation of perfumes, soaps, flavourings" (1). Coumarins are attaining importance, for the reason that they have varied biological activities and less toxicity. The derivatives of coumarin have many pharmacological activities like anti-inflammatory, antiviral, antioxidant, antiallergic, hepatoprotective, antithrombotic and anticarcinogenic (2). "Coumarin derivatives are widely used as rodenticides due to the property of causing fatal hemorrhaging" (Sancheti et al. 2013). Moreover coumarin derivatives are used for reversal of multidrug resistance of bacteria and cancer cells.

When the methyl group attached to coumarin structure at 7 position, 7-Methylcoumarin (7MC) is obtained. 7MC is white, crystalline powder, obtainable naturally from several plants. In the literature, the lethal toxic dose is reported for 7MC as 3,800 mg/kg (Hoult et al. 1996). And also 7MC has strong hepatoprotective activity and this attributes to its potent antioxidant effects. 7MC eliminates significantly the E-coli plasmid (Shah et al. 1998). Accordingly, 7MC is an important coumarin derivatives.

Received 14 December 2020, Accepted 17 December 2020, Available online 18 December.

In order to understand the relationship between pharmacological activity and molecular structure, the knowledge of their conformational distribution and spectral properties are especially important. So, authors studied molecular structure and spectral properties of some coumarin derivatives before (Sarikaya et al. 2013a and 2013b). This time, the same studies were performed for 7MC in this study.

2. Materials and methods

Similar to our previous coumarin studies (Sarikaya et al. 2013a and 2013b), the 7MC powder was purchased from ABCR Specialty Chemicals for Research, Development and Production Company and the experimental part of this study was performed by the same way. "FT-IR spectrum of solid 7MC was recorded in the range 4000–400 cm^{-1} on Brucker IFS 66/S with PIKE Gladi ATR (Diamond) spectrometer at room temperature with 2 cm^{-1} resolutions. The FT-Raman spectrum was recorded on a Brucker FRA 106/S spectrometer using 1064 nm excitation from a Nd: YAG laser. The detector was a Gediode cooled to liquid nitrogen temperature. The upper limit for wavenumbers was 3500 cm^{-1} and the lower wavenumber is around 50 cm^{-1}. The measured FT-IR and FT-Raman spectra are shown in Figures 1 and 2. (Sarikaya et al. 2013b and 2014).

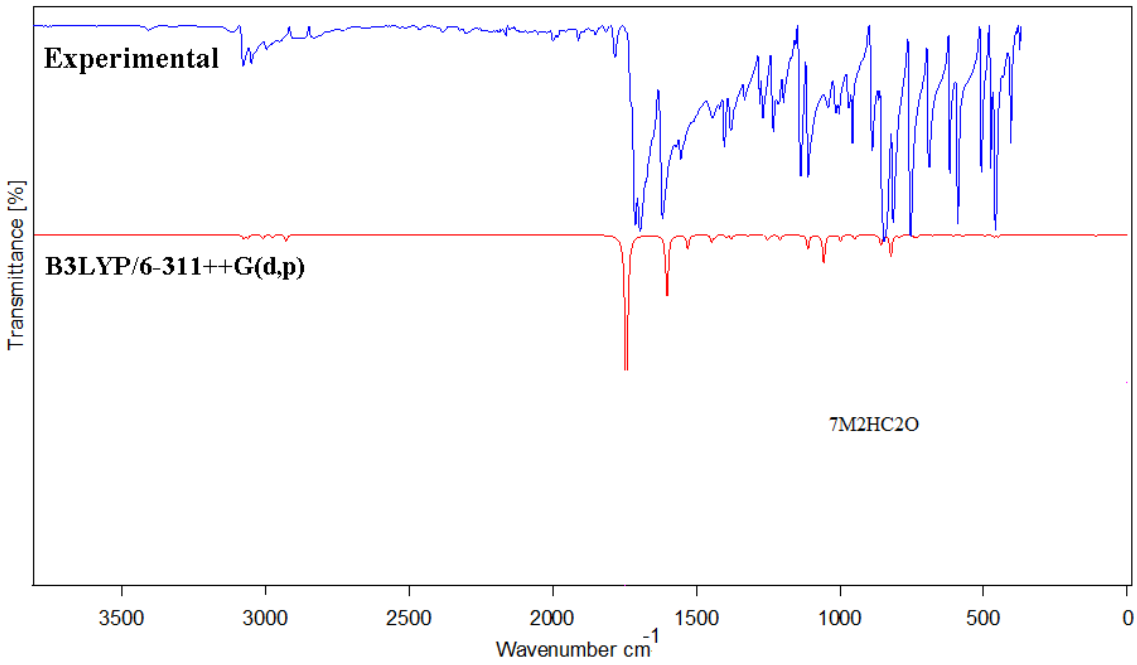

Figure 1. Experimental and theoretical FT-IR spectra of 7-Methylcoumarin molecule.

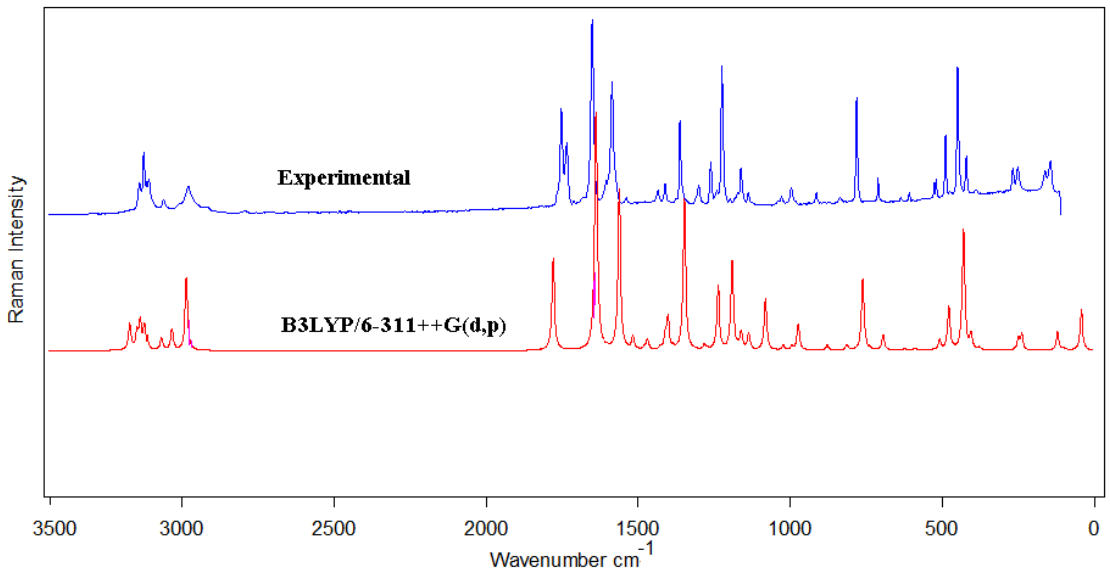

Figure 2. Experimental and theoretical FT-Raman spectra of 7-Methylcoumarin molecule.

Geometry parameters of the molecule that we worked is not in the literature, with the aim of finding a stable structure made of conformational analysis. Conformational distribution of molecule obtained by scanning the potential energy surface were determined using the program Spartan 08 (Spartan 2018). To do this, Merck Molecular Force Field (MMFF) (Halgren 1996) method was used for. After determining all conformations to identify the most stable conformation, geometry optimization calculations were performed with the Gaussian 16W (Gaussian 2016) program.

Furthermore for the vibrational frequency calculations and calculations of other properties of molecule GaussView 6.0 graphical interface was carried out with Gaussian 16W program. In all calculations such as geometry optimization, vibrational frequency and other molecular property calculations were performed by B3LYP (Becke 1988 and 1993; Le et al. 1988) functional and 6-311++G(d,p) and cc-pVDZ basis set. Fundamental vibrational modes of the total energy distribution (TED) calculations and Scaled quantum mechanics (SQM) method with Parallel Quantum Solutions (PQS) program (SQM 2013) has been utilized. Additionally, Raman İntensities were calculated by RaInt (Michalska 2003) programs.

NMR analysis has been done by using Gauge Independent Atomic Orbital (GIAO) method. The ^{1}H and ^{13}C NMR spectra calculations were performed by Gaussian 16W program package. The ^{1}H and ^{13}C NMR chemical shifts calculations of the 7MC molecule were made by using B3LYP functional with 6-311++G(d,p) basis set. The calculations were performed in chloroform solution by using IEF-PCM model. Results compared with experimental results for the identification and characterization of 7MC molecule.

3. Results and discussion

Conformational stability and molecular structure

A careful conformational analysis was executed for the sample when determining the stable conformation. The free rotation bonds were rotated 10 degrees around itself in conformational space

of 7MC which is scanned with semi empirical MMFF method (Halgren 1996) Consequences of conformational analysis indicated that the title compound has only one stable conformer. Afterwards full geometry optimizations calculations of title compound were carried out by B3LYP/6-311++G(d,p) and cc-pVDZ level. The optimized structure of conformer of 7MC was shown in Figure 3 which has the atom numbering scheme adopted in this study. Take a look at Table 1 as follows, ground state energies, zero point corrected energies ($E_{elect.}$ + ZPE), relative energies and dipole moments of the conformer were observed.

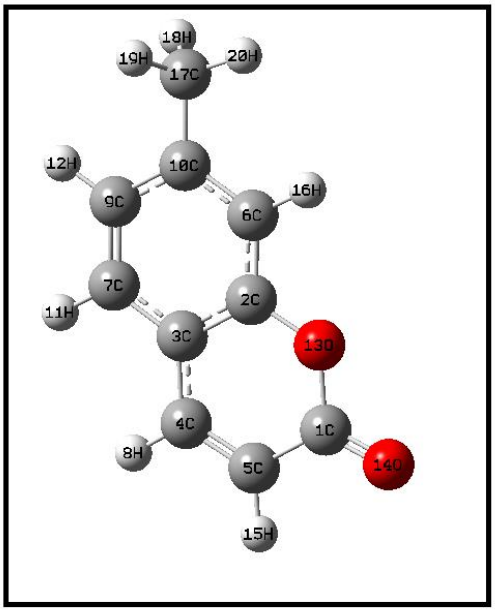

Figure 3. Molecular structure and atomic numbering of 7-Methylcoumarin molecule.

Table 1. Energetics of the conformer calculated at the B3LYP/6-311++G(d,p) level

Conf.	***E* (Hartree)**
1	-536.485865

E_o- Zero point corrected energy

The optimized structural parameters such as dihedral angles, bond angles and bond lengths of the 7MC conformer was given in Table 2. Because there was no any information about the molecular structure of 7MC in the literature, in this study, the calculated structural parameters of 7MC was compared with closely related molecule tert-Butyl Coumarin-3-carboxylate (Yavari 2006). Because the experimental section of this study belong to solid phase while theoretical part belongs to gaseous phase, the observation of small differences between experimental and calculated geometrical parameters are reasonable.

Table 2. The calculated geometric parameters of 7-Methylcoumarin by B3LYP/6-311++G(d,p) and B3LYP/cc-pVDZ method, bond lengths in angstrom (Å) and angles in degrees(^{0}).

Parameters	Calculated		Experimental[a]	Parameters	Calculated		Experimental[a]
Bond lengths	**cc-pVDZ**	**6-311++G(d,p)**		**Bond angles**	**cc-pVDZ**	**6-311++G(d,p)**	
C_1-C_5	1.461	1.457	1.464	C_{10}-C_{17}-H_{20}	111.6	111.5	-
C_1-O_{13}	1.401	1.398	1.383	H_{18}-C_{17}-H_{19}	106.9	107.2	-
C_1-O_{14}	1.205	1.203	1.201	H_{18}-C_{17}-H_{20}	108.0	108.0	-
C_2-C_3	1.408	1.403	1.394	H_{19}-C_{17}-H_{20}	108.0	108.0	-
C_2-C_6	1.399	1.394	1.389	**Dihedral angles**			
C_2-O_{13}	1.363	1.364	1.368	O_{13}-C_1-C_5-C_4	0.00	0.0	0.82
C_3-C_4	1.441	1.438	1.429	O_{13}-C_1-C_5-H_{15}	180.0	179.9	-
C_3-C_7	1.410	1.407	1.403	O_{14}-C_1-C_5-C_4	180.0	179.9	178.65
C_4-C_5	1.354	1.350	1.355	O_{14}-C_1-C_5-H_{15}	0.0	0.0	-
C_4-H_8	1.093	1.086	0.949	C_5-C_1-O_{13}-C_2	0.0	0.0	0.68
C_5-H_{15}	1.090	1.082	-	O_{14}-C_1-O_{13}-C_2	180.0	180.0	178.89
C_6-C_{10}	1.396	1.392	1.381	C_6-C_2-C_3-C_4	180.0	180.0	179.43
C_6-H_{16}	1.091	1.084	0.949	C_6-C_2-C_3-C_7	0.0	0.0	1.25
C_7-C_9	1.386	1.382	1.379	O_{13}-C_2-C_3-C_4	0.0	0.0	1.2
C_7-H_{11}	1.092	1.085	0.950	O_{13}-C_2-C_3-C_7	180.0	179.9	178.09
C_9-C_{10}	1.412	1.409	1.406	C_3-C_2-C_6-C_{10}	0.0	0.0	0.97
C_9-H_{12}	1.092	1.085	0.949	C_3-C_2-C_6-H_{16}	179.9	180.0	179
C_{10}-C_{17}	1.508	1.508	-	O_{13}-C_2-C_6-C_{10}	180.0	179.9	178.4
C_{17}-H_{18}	1.102	1.094	-	O_{13}-C_2-C_6-H_{16}	0.0	0.0	1.61
C_{17}-H_{19}	1.102	1.094	-	C_3-C_2-O_{13}-C_1	0.0	0.0	0.36
C_{17}-H_{20}	1.099	1.091	-	C_6-C_2-O_{13}-C_1	180.0	180.0	179.74
Bond angles				C_2-C_3-C_4-C_5	0.0	0.0	1
C_5-C_1-O_{13}	115.9	115.9	116.6	C_2-C_3-C_4-H_8	180.0	180.0	179.04
C_5-C_1-O_{14}	126.4	126.4	127.4	C_4-C_3-C_7-C_9	179.9	180.0	179.72
O_{13}-C_1-O_{14}	117.5	117.7	115.9	C_7-C_3-C_4-H_8	0.0	0.0	1.68
C_3-C_2-C_6	121.1	121.4	121.5	C_3-C_4-C_5-C_1	0.0	0.0	0.03
C_3-C_2-O_{13}	121.5	121.3	121.1	C_2-C_3-C_7-H_{11}	179.9	179.9	179.55
C_6-C_2-O_{13}	117.2	117.3	117.3	C_2-C_6-C_{10}-C_9	0.0	0.0	0.08
C_2-C_3-C_4	117.4	117.5	117.3	C_4-C_3-C_7-H_{11}	0.0	0.0	0.29
C_2-C_3-C_7	118.0	118.0	118.8	C_2-C_6-C_{10}-C_{17}	179.9	179.9	-
C_4-C_3-C_7	124.4	124.5	123.8	C_3-C_4-C_5-H_{15}	180.0	180.0	-
C_3-C_4-C_5	120.6	120.8	121.9	H_8-C_4-C_5-C_1	180.0	179.9	179.91
C_3-C_4-H_8	118.8	118.8	119	H_8-C_4-C_5-H_{15}	0.0	0.0	-
C_5-C_4-H_8	120.5	120.4	118.9	C_3-C_7-C_9-C_{10}	0.0	0.0	0.56
C_1-C_5-C_4	121.7	121.6	119.9	C_7-C_9-C_{10}-C_6	0.0	0.0	0.85
C_1-C_5-H_{15}	115.4	115.6	-	H_{16}-C_6-C_{10}-C_9	179.9	179.9	179.92
C_4-C_5-H_{15}	122.7	122.8	-	H_{16}-C_6-C_{10}-C_{17}	0.0	0.0	-
C_2-C_6-C_{10}	120.2	120.1	118.7	C_7-C_9-C_{10}-C_{17}	179.9	179.9	-
C_2-C_6-H_{16}	118.3	118.6	120.6	C_3-C_7-C_9-H_{12}	179.9	179.9	179.44
C_{10}-C_6-H_{16}	121.3	121.3	120.6	H_{11}-C_7-C_9-C_{10}	180.0	179.9	179.41
C_3-C_7-C_9	120.7	120.7	120.3	H_{11}-C_7-C_9-H_{12}	0.0	0.0	0.57
C_3-C_7-H_{11}	118.8	119.0	119.8	C_7-C_3-C_4-C_5	0.0	179.9	178.26
C_9-C_7-H_{11}	120.3	120.3	119.8	C_2-C_3-C_7-C_9	0.0	0.0	0.46
C_7-C_9-C_{10}	120.8	120.9	119.5	H_{12}-C_9-C_{10}-C_6	179.9	179.9	179.15
C_7-C_9-H_{12}	119.7	119.8	120.2	H_{12}-C_9-C_{10}-C_{17}	0.0	0.0	-
C_{10}-C_9-H_{12}	119.3	119.4	120.2	C_6-C_{10}-C_{17}-H_{18}	120.6	120.5	-
C_6-C_{10}-C_9	118.8	118.9	120.9	C_6-C_{10}-C_{17}-H_{19}	120.5	120.4	-
C_6-C_{10}-C_{17}	120.9	120.9	-	C_6-C_{10}-C_{17}-H_{20}	0.03	0.0	-
C_9-C_{10}-C_{17}	120.2	120.2	-	C_9-C_{10}-C_{17}-H_{18}	59.37	59.49	-
C_1-O_{13}-C_2	122.6	122.9	122.9	C_9-C_{10}-C_{17}-H_{19}	59.43	59.55	-
C_{10}-C_{17}-H_{18}	110.9	111.0	-	C_9-C_{10}-C_{17}-H_{20}	179.9	179.9	-
C_{10}-C_{17}-H_{19}	110.9	111.0	-				

[a]Values are taken from Ref. [16]

Vibrational assignments

A molecule, consisting of 20 atoms, has 54 normal modes of vibrations which are active in both infrared and Raman spectra. In this study, harmonic vibrational wavenumbers of the tittle compound were calculated by B3LYP/6-311++G(d,p) and cc-pVDZ level of theory. It is known that these wavenumbers must be scaled by a proper scale factor because of the anharmonicity of the incomplete treatment of electron correlation and of the use of finite one-particle basis set. There are scaled factors for calculated harmonic vibrational wavenumbers in literature (Young 2001). Subsequently the calculated harmonic frequencies scaled by 0.967 for wave numbers under 1800 cm^{-1} and 0.955 for those over 1800 cm^{-1} for B3LYP/6-311++G(d,p). Additionally, the harmonic frequencies calculated at cc-pVDZ level were scaled by 0.970 (NIST; Erdogdu et al. 2010; Dereli et al. 2012). As it is seen in Table 3 which the experimental and the calculated values are gathered, the calculated values are in good agreement with the experimental values.

Table 3. Comparisons of the observed and calculated vibrational spectra of 7-Methylcoumarin.

Mode Nos.	Experimental wavenumbers(cm^{-1})		Theoretical wavenumbers (cm^{-1})				TED[b](%)
			B3LYP/6-311++G(d,p)			B3LYP/cc-pVDZ	
	IR	Raman	Scaled[a]	I_{IR}	I_{Raman}	Scaled[a]	
ν_1	3117	-	3109	0	16	3127	97 ν(CH), pyr
ν_2	-	-	3086	0	10	3104	99 ν_s (CH), ring
ν_3	3077	3076	3075	2	17	3094	98 ν_s(CH),ring
ν_4	3070	3064	3062	2	12	3079	97 ν_{as}(CH), pyr ring
ν_5	3048	3052	3059	0	3	3077	99 ν_{as}(CH), pyr ring
ν_6	2996	3005	3008	2	7	3031	100 $\nu_{as}(CH_3)$
ν_7	2950	2970	2974	2	13	2996	100 $\nu_{as}(CH_3)$
ν_8	2925	2921	2927	3	43	2940	100 $\nu_s(CH_3)$
ν_9	1713	1718	1743	100	56	1781	84 ν(C=O)
ν_{10}	-	-	1604	8	58	1624	66 ν(C=C) pyr + 11δCCH pyr
ν_{11}	1616	1617	1601	25	100	1618	61 ν(C=C) ring + 12δCCH ring
ν_{12}	1554	1556	1530	7	96	1547	67 ν(C=C) pyr ring
ν_{13}	-	-	1485	0	8	1493	44 ν(C=C) pyr ring + 39δCCH pyr ring
ν_{14}	1444	-	1446	3	2	1430	83 $\delta(CH_3)$
ν_{15}	1419	-	1436	1	6	1411	90 $\delta(CH_3)$
ν_{16}	1402	-	1395	1	1	1395	30 δCCH pyr ring +28ν(C=C) pyr ring
ν_{17}	1380	1380	1378	2	8	1377	54 δCCH pyr ring +26ν(C=C) pyr ring
ν_{18}	-	-	1369	0	19	1354	96 $\delta_s(CH_3)$, umbrella
ν_{19}	1332	1336	1319	1	90	1343	77 ν(C=C) ring
ν_{20}	1268	1275	1253	3	3	1259	50 δCCH ring +22ν(C=C) ring +10ν(OC) pyr
ν_{21}	1232	1234	1243	1	1	1237	47 δCCH pyr, ring +12ν(C=C) pyr, ring +11ν(OC) pyr
ν_{22}	1214	1215	1208	3	38	1212	52 ν(C=C) pyr ring + 21δCCH pyr ring
ν_{23}	1155	-	1162	0	53	1158	49 δCCH pyr, ring +32ν(C=C) pyr, ring
ν_{24}	1137	1139	1136	0	10	1132	54 δCCH pyr, ring +28ν(C=C) pyr, ring
ν_{25}	1111	1116	1111	7	10	1115	35 δCCH pyr, ring +23ν(OC) pyr +16ν(C=C) pyr, ring
ν_{26}	1041	-	1056	14	30	1066	37 δCCH pyr +29ν(C=C) pyr +21ν(OC) pyr
ν_{27}	1014	-	1023	1	0	1017	95 $\delta(CH_3)$, rocking
ν_{28}	1003	-	998	3	3	993	64 $\delta(CH_3)$, rocking +13ν(C=C) ring
ν_{29}	969	973	970	0	3	985	89 γ(CH), pyr
ν_{30}	957	954	948	2	16	948	21 δCCH ring +19ν(C=C) ring + 10δCCC ring+10ν(OC) pyr
ν_{31}	921	-	934	0	0	944	88 γ(CH), ring
ν_{32}	846	-	859	1	0	876	80 γ(CH), ring
ν_{33}	-	-	857	4	3	859	29 ν(OC) pyr +16ν(C=C) pyr+16 δCCC pyr+12δCCH
ν_{34}	815	-	823	10	0	836	76 γ(CH), pyr ring
ν_{35}	793	-	793	1	3	799	24 ν(C=C) pyr ring +15ν(CC) +13 ν(OC) pyr +11 δCCC pyr
ν_{36}	-	-	787	0	0	796	85 γ(CH) pyr ring
ν_{37}	754	763	740	1	42	754	44 ν(C=C) ring +18ν(OC) pyr
ν_{38}	730	-	730	1	1	744	35 τ CCCC +12 τ CCOC +12 τ CCCO
ν_{39}	688	695	677	0	9	679	30 δCCC +19 ν(C=C) +15 ν(CC)
ν_{40}	-	-	666	0	0	678	21 τ CCCH +18 τ CCCC +16 τ HCCO
ν_{41}	618	-	606	1	1	606	32 δCCC +13 δCCO +11 δOCO

ν_{42}	590	592	572	1	1	588	25 τ CCCH +22 τ CCCC
ν_{43}	508	510	495	1	6	494	35 δCCO +17 δOCO +13 δCCC
ν_{44}	475	478	464	1	26	464	35 δCCC +23 δCCO
ν_{45}	459	-	450	1	0	456	38 τ CCCC +18 τ CCCH
ν_{46}	405	410	416	0	72	417	20 δCCC +15 ν(C=C) +14 ν(OC) +10 δCCO
ν_{47}	386	377	391	0	9	399	44 τ CCCC +10 τ CCCO
ν_{48}	374	-	364	0	1	363	60 δCCC +11 δCCO
ν_{49}	-	-	248	0	0	257	37 τ CCCC +27 τ CCCO
ν_{50}	-	261	239	0	7	245	38 τ CCCC +29 τ CCCO
ν_{51}	-	243	228	0	10	228	48 δCCC+20 δCCO
ν_{52}	-	106	110	1	11	115	47 τ CCCC +15 τ CCCO
ν_{53}	-	-	91	0	1	95	23 τ COCC +21 τ CCCO +18τ COCO +11 τ CCCC
ν_{54}	-	40	36	0	24	55	97 τ(CH_3)

υ, stretching; *δ*, in-plane bending; *γ*, out-of-plane bending ; τ torsion

Relative absorption intensities and Raman intensities normalized with highest peak absorption equal to 100.

[a] Obtained from the wave numbers calculated at B3LYP/6-311++G(d,p) using scaling factors 0.967 (for wave numbers under 1800 cm^{-1}) and 0.955 (for those over 1800 cm^{-1}) and at B3LYP/cc-pVDZ using scaling factors 0.970.

[b] Total energy distribution calculated B3LYP/6-311++G(d,p) level of theory. Only contributions ≥10% are listed.

As a well-known knowledge of literature, CH stretching and in plane bending vibrations are observed in the 3100–3000 cm^{-1} and 1100–1500 cm^{-1} region, respectively while the out-of-plane bending vibrations occur in the wavenumber range 800–1000 cm^{-1} (Varsayani 1973; Jag 2001; Du et al. 2002).

The aromatic C–H stretching vibrations of the title compound were observed at 3117, 3077, 3070 and 3048 cm^{-1} in FT-IR spectrum and at 3076, 3064 and 3052 cm^{-1} in FT-Raman spectrum (mode nos.: 1, 2, 3, 4 and 5). All predicted wavenumbers of CH stretching vibrations well reproduced the experimental ones in the infrared and Raman spectrum. The theoretical values predicted by 6-311++G(d,p) and cc-pVDZ level at 3109, 3086, 3075, 3062, 3059 cm^{-1} and 3127, 3104, 3094, 3079, 3077 cm^{-1}, respectively were well correlated with experimental values. As shown in Table 3, these values were almost the same.

The in-plane CH bending vibrations of rings were observed at 1380, 1268, 1232, 1155 and 1137 cm^{-1} in FT-IR spectrum and the bands at 1380, 1275, 1234 and 1139 cm^{-1} in FT-Raman spectrum (mode nos:17,20,21,23,24). The in plane CH bending vibrations are calculated by B3LYP/6-311++G(d,p) level at 1378, 1253, 1243, 1162, 1136 cm^{-1} and by B3LYP/cc-pVDZ 1377, 1259, 1237, 1158, 1132 cm^{-1}.

The bands observed at 969, 921, 846 and 815 cm^{-1} in the FT-IR spectrum (mode nos:29, 31, 32, 34 and 36) and the band observed at 973 cm^{-1} in the Raman spectrum were assigned to out-of-plane CH vibrations. The computed wave number for out-of-plane CH vibrations are obtained at 985, 944, 876, 836, 796 cm^{-1} by B3LYP/cc-pVDZ and obtained at 970, 934, 859, 823, 787 cm^{-1} by 6-311++G(d,p) level. These results show us the harmony between the calculated and the experimental wave numbers of in-plane and out-of-plane CH bands.

"For the assignments of CH_3 group frequencies, nine fundamental vibrations can be associated to each CH_3 group. Three stretching, three bending, two rocking modes and a single torsional mode describe the motion of the methyl group (Bahgat 2006). "The most useful diagnostic bands to determine the presence of methyl or methylene groups in a sample are the C-H stretching vibrations that these groups exhibit. These vibrations typically fall between 2800 and 3000 cm^{-1}" (Smith 1998). In the FT-IR spectrum of title compound, the antisymmetric stretching modes of CH_3 are observed at 2996 and 2950 cm^{-1}. The counter part of the Raman spectrum at 3005 and 2970 cm^{-1} are attributed to CH_3 antisymmetric stretching vibrations. The wave number computed at 3008, 2974 cm^{-1} by B3LYP/6-311++G(d,p) and at 3031, 2996 cm^{-1} by B3LYP/cc-pVDZ level are assigned to the CH_3 antisymmetric stretching vibrations (mode nos:6,7). The symmetrical stretching mode of CH_3 is observed at 2925 cm^{-1} in FT-IR spectrum and 2921 cm^{-1} in Raman spectrum. The theoretically calculated CH_3 symmetric stretching vibrations by B3LYP/6-311++G(d,p) and

B3LYP/cc-pVDZare 2927 cm^{-1} and 2940 cm^{-1} (mode no:8), respectively. The calculated wave number is exactly correlated with this number.

The bands observed at 1444 and 1419 cm^{-1} in the FT-IR spectrum were assigned to deformation bending. The theoretically computed values by B3LYP/6-311++G(d,p) and B3LYP/cc-pVDZ level are at 1446, 1436 and 1430, 1411 cm^{-1} respectively for deformation bending (mode nos: 14,15). And the band observed at 1014 and 1003 cm^{-1} in the FT-IR were assigned to rocking vibrations of CH_3. The computed 6-311++G(d,p) and cc-pVDZ values are at 1023, 998 and 1017, 993 cm^{-1} respectively, for rocking vibrations (mode nos: 27,28). However the symmetric bending vibrations didn't observed in FT-IR and Raman spectrum, the theoretically calculated symmetric bending vibration was at 1369 cm^{-1} by 6-311++G(d,p) and at 1354 cm^{-1} by cc-pVDZ (mode no:18). The Raman band observed at 40 cm^{-1} was assigned to torsional vibration of CH_3 group (mode no:54). In the CH_3 part of this study, the calculated wavenumbers and the experimantal counterparts of them has good correlation with the literature data (Udaya et al. 2012; Moghanian et al. 2013; Mishra et al. 2013).

Usually carbonyl group vibrations occur in the region 1780-1700 cm^{-1} (Sajan et al. 2011; Erdogdu 2011). In our paper, the band appeared at 1713 cm^{-1} (FT-IR) and 1718 cm^{-1} (FT-Raman) are belongs to C=O group (mode no:9). The C_1-O_{13} and C_2-O_{13} stretching frequencies in coumarin derivatives were assigned from 850 cm^{-1} to 1250 cm^{-1} (Smith 1998; Sajan et al. 2011; Erdogdu 2011) in the literature. In our study these vibrations were observed at 1111 cm^{-1} (1116 cm^{-1} in Raman) and 1041 cm^{-1} in FT-IR spectrum. The wave numbers computed by 6-311++G(d,p) and cc-pVDZat 1111, 1056 and 1115, 1066 cm^{-1}, respectively show better agreement with the experimental values (mode nos:25,26), which were assigned to the CO stretching vibrations.

In the literature, the C-C ring stretching vibrations of other coumarin derivatives were found in the region 1600–740 cm^{-1} (Bahgat 2006; Sajan et al. 2011; Ramoji et al. 2007). The bands observed at 1616, 1554, 1332, 1214, 793 and 754 cm^{-1} in FT-IR spectrum and at 1617, 1556, 1336, 1215 and 763 cm^{-1} in Raman spectrum (mode nos: 10,11,12,13,19,22,35,37) were assigned to C-C stretching vibrations.

NMR Spectra

Here, we given an application of ^1H and ^{13}C NMR experimental and theoretical molecular modeling approach. The ^1H and ^{13}C NMR spectrum for 7MC is summarized in Table 4. As seen in Figure 4, the theoretically generated ^1H NMR and ^{13}C NMR spectra correlate well with the experimental spectra. The observed NMR spectra were explained on the basis of the calculated NMR chemical shifts in chloroform for 7MC. The NMR spectra calculations were performed for chloroform solvent. The isotropic shielding values were used to calculate the isotropic chemical shifts δ with respect to tetramethylsilane (TMS) ($\delta_{iso}^{X} = \sigma_{iso}^{TMS} - \sigma_{iso}^{X}$) (Erdogdu 2013; Alkorta et al. 1996).

Table 4. Theoretical and experimental ^{1}H and ^{13}C spectra of the most stable of 7-Methylcoumarin molecule (with respect to TMS. all values in ppm).

Atom	B3LYP 6-311++G(d.p)	Exp.	Atom	B3LYP 6-311++G(d.p)	Exp.
C_1	160.9	160.9	H_8	7.68	7.67
C_2	161.4	154.2	H_{11}	7.47	7.36
C_4	148.7	143.3	H_{16}	7.24	7.11
C_{10}	150.3	143.0	H_{12}	7.27	7.09
C_7	131.7	127.5	H_{15}	6.11	6.34
C_9	128.4	125.5	H_{18}-H_{19}	2.56	2.44
C_6	120.5	117.0	H_{20}	2.04	2.44
C_3	120.1	116.5			
C_5	117.6	115.4			
C_{17}	22.03	21.71			

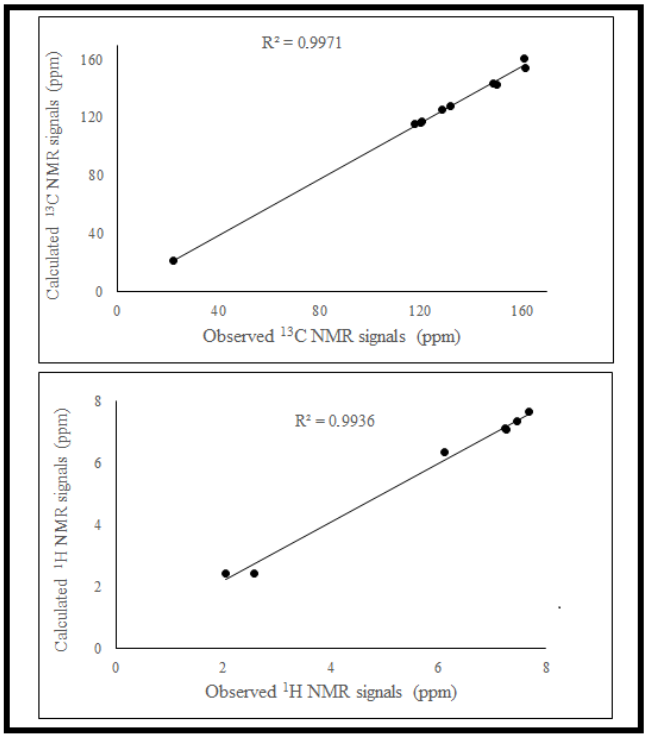

Figure 4. Correlation plot between calculated and experimental Carbon and Proton NMR signals by B3LYP/6-311++G(d,p).

The ^{13}C NMR chemical shifts of coumarin ring were measured in the 117 ppm-160 ppm region. The ^{13}C NMR chemical shifts for organic molecule usually is higher than 100 ppm, as reported in the literature (Subashchandrabose et al. 2010; Joseph et al. 2012; Erdogdu et al. 2009; Gulluoglu et al. 2011). These are clearly found in the expected regions.

Zolek et al. (Zolek et al. 2003) published that the ^{13}C CP MAS NMR spectra were experimental obtained for a series of 11 solid coumarin with chloroform solution. The ^{13}C chemical shifts of these compounds were determined by Zolek et al. (Zolek et al. 2003). Chemical shifts of Carbon-1 were observed at 160.4 ppm by Zolek (Zolek et al. 2003). In this work, the signal at 162.63 ppm was assigned to the C_1 carbon. This signal was predicted at 160.9 ppm for B3LYP/6-311++G(d,p) level of theory. The NMR signals of C_2, C_3, C_4, C_5, C_6, C_7 and C_9 were determined at

154.2 ppm (161.4 ppm //B3LYP/6-311++G(d,p)), 116.5 ppm (120.1 ppm //B3LYP/6-311++G(d,p)), 143.3 ppm (148.7 ppm //B3LYP/6-311++G(d,p)), 115.4 ppm (117.6 ppm //B3LYP/6-311++G(d,p)), 117.0 ppm(120.5 ppm //B3LYP/6-311++G(d,p)), 127.5 ppm (131.7 ppm //B3LYP/6-311++G(d,p)) and 125.5 ppm (128.4 ppm //B3LYP/6-311++G(d,p)) by experimental, respectively.

The NMR signal of Carbon-10 in 7MC was resonated at 143.3 ppm. In the theoretical approach, this signal was calculated at 150.3 ppm by B3LYP/6-311++G(d,p) level of theory. This carbon atom is attached to the methyl groups. Carbon peak of the methyl group was detected at 22.03 ppm. The CH_3 groups are generally showed as electron donating groups, so they will be more shielded. The experimental chemical shifts of protons attached to CH_3 group are detected higher magnetic field. The computed chemical shifts as well as experimental NMR values are shown in Table 4.

The predicted and measured ^{1}H NMR spectrum of 7MC founded eight signals in the aromatic region. Five of these signals were determined to the coumarin group. In ^{1}H NMR spectra of 7MC molecule, these peaks resonated in the gap 7.67–6.34 ppm for the H atoms of coumarin ring. The other three signals were assigned to the methyl group. The peaks of H atoms of methyl group are smaller than those of coumarin ring. ^{1}H NMR signals of CH_3 group were experimentally resonated at 2.44 ppm (H_{18}, H_{19} and H_{20}) ppm. The calculated chemical shift values for the CH_3 proton were 2.56 ppm (H_{18} and H_{19}) and 2.04 ppm (H_{20}) for B3LYP/6-311++G(d,p) level of theory.

Frontier molecular orbital analysis

To study the reactivity of 7MC and to predict its behavior in the gas phase, the frontier HOMO–LUMO molecular orbitals and electronegativity (χ), electron affinity (E_A), ionization potential (I_P) and chemical hardness (η) were calculated at the B3LYP/cc-pVDZ level of theory. These data were summarized in the Table 5.

$$IP \approx -E_{HOMO}$$

$$EA \approx -E_{LUMO}$$

$$\eta = (E_{LUMO} - E_{HOMO})/2$$

$$\chi = (E_{LUMO+} E_{HOMO})/2$$

The calculated eigen values of LUMO and HOMO are -1.915 eV and -6.451 eV, respectively while their energy gap is 4.516 eV. The plot of HOMO and LUMO are illustrated in Figure 5.

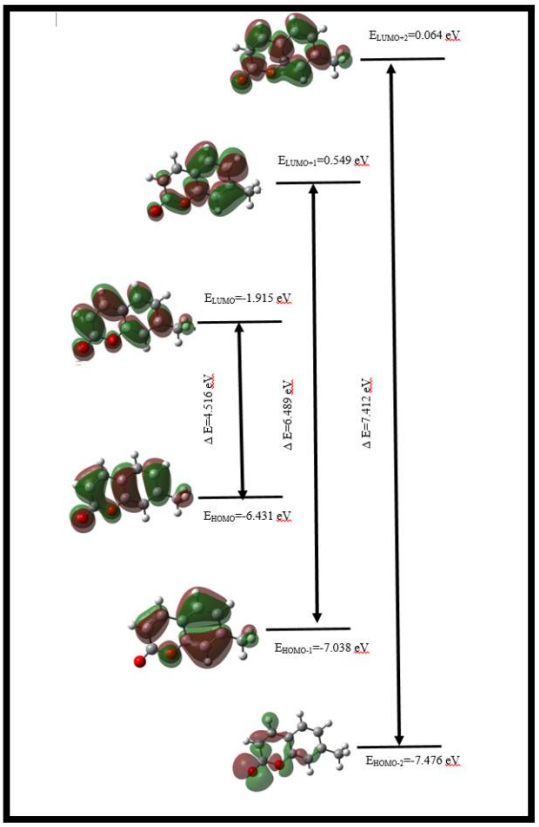

Figure 5. HOMO-LUMO plot of 7-Methylcoumarin molecule by B3LYP/cc-pVDZ level of theory.

Table 5. Calculated some properties values of 7-Methylcoumarin in its ground state (B3LYP/cc-pVDZ).

E_{HOMO} (eV)	-6.431
ΔE_{GAP} (eV)	4.516
E_{LUMO} (eV)	-1.915
E_{HOMO-1} (eV)	-7.038
$\Delta E_{GAP\ 1}$ (eV)	6.489
E_{LUMO+1} (eV)	-0.549
E_{HOMO-2} (eV)	-7.476
$\Delta E_{GAP\ 2}$ (eV)	7.412
E_{LUMO+2} (eV)	-0.064
IP (eV)	6.431
EA (eV)	1.915
η (eV)	2.258
χ (eV)	4.173

Molecular electrostatic potential maps

The MEP maps of the most stable state of 7MC was given in Figure 6. The molecular electrostatic potential (MEP) is usually used as a reactivity map displaying most probable regions for the electrophilic attack of charged point-like reagents on organic molecules. MEP contour map provides a simple way to predict how different geometries could interact. The calculated 3D MEP

contour map (red is negative, blue is positive) shows the negative regions are mainly over the Oxygen atoms. As we have mentioned earlier, the electrostatic potential has been used primarily for predicting sites and relative reactivities towards electrophilic attack.

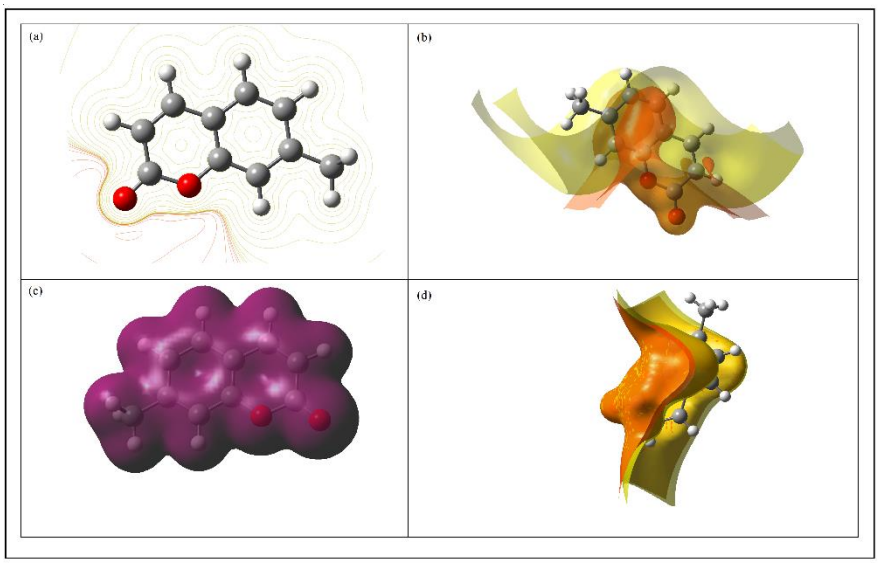

Figure 6. Molecular electrostatic potential mapped (a, b and d) and electron density (C) of 7-Methylcoumarin molecule by B3LYP/cc-pVDZ level of theory.

4. Conclusions

The equilibrium geometries, harmonic wavenumbers, ground state energies, and dipole moments and vibrational band assignments of this conformer of 7MC have been given for the first time in this study. The calculated vibrational frequencies of conformer have been found in good agreement with IR and Raman experimental data. This shows that the obtained structures were very close to real structure of 7MC.

References

Alkorta I, Perez JJ, (1996) Molecular polarization potential maps of the nucleic acid bases. Int. J. Quantum Chem 57: 123–135.

Bahgat K, (2006) Scaled quantum chemical studies of the structural and vibrational spectra of acetyl coumarin. Central Eur. J. Chem. 4 (4): 773–785.

Becke AD (1988) Density-functional exchange-energy approximation with correct asymptotic behavior. Phys Rev A 38:3098–3100.

Becke AD (1993) Density-functional thermochemistry. III. The role of exact exchange. J Chem Phys 98:5648–5652.

Dennington R, Keith TA, Millam JM, GaussView, Version 6, Semichem Inc., Shawnee Mission, KS, 2016.

Dereli Ö, Erdogdu Y, Gulluoglu MT, Türkkan E, Özmen A, Sundaraganesan N, (2012) Vibrational Spectral and Quantum Chemical Investigations of Tert-butyl-hydroquinone. J. Mol. Struct 1012: 168-176.

Du XH, Hansell C, Doyle EPS, Caffrey CR, Holler TP, McKerrow JH, Cohen FE, (2002) Optimization of Blood–Brain Barrier Permeability with Potent and Selective Human Neuronal Nitric Oxide Synthase Inhibitors Having a 2-Aminopyridine Scaffold. J. Med. Chem 45: 2690–2707.

Erdogdu Y, (2013) Investigations of FT-IR, FT-Raman, FT-NMR spectra and quantum chemical computations of Esculetin molecule Spectrochim. Acta A: Mol. Biomol. Spectroscn 106: 25-33

Erdogdu Y, Güllüoğlu MT, Kurt M, (2009) DFT, FT-Raman, FT-IR and NMR studies of 2-Fluorophenylboronic Acid J. Raman Spect 40(11): 1615-1623.

Erdoğdu Y, Unsalan O, Amalanathan M, Joe IH, (2010) Infrared and Raman Spectra, Vibrational Assignment, NBO Analysis and DFT Calculations of 6-Aminoflavone. J. Mol. Struct., 980: 24-30.

Frisch MJ. et all., Gaussian 16, Revision B.01, Gaussian, Inc., Wallingford CT, 2016.

Güllüoğlu M T, Erdogdu Y, Karpagam J, Sundaraganesan N, Yurdakul Ş, (2011) DFT, FT-Raman, FT-IR and FT-NMR studies of 4-phenylimidazole J. Mol. Struct 990: 14-20.

Halgren TA, (1996) Merck molecular force field. I. Basis, form, scope, parameterization, and performance of MMFF94. J Comput Chem. 17: 490–519.

Hoult JRS, Payá M, (1996) Pharmacological and biochemical actions of simple coumarins: Natural products with therapeutic potential. Gen Pharmacol. 27: 713-722.

http://chemicalland21.com/lifescience/uh/methylcoumarin.htm

http://en.wikipedia.org/wiki/Coumarin

Jag M, (2001) Organic Spectroscopy – Principles and Alications, second ed., Narosa Publishing House, New Delhi.

Joseph L, Sajan D, Reshmy R, Sasi BSA, Erdogdu Y, Thomas KK, (2012) Vibrational spectra, structural conformations, scaled quantum chemical calculations and NBO analysis of 3-acetyl-7-methoxycoumarin. Spectrochim. Acta 99: 234-247.

Lee C, Yang W, Parr RG (1988) Development of the Colle-Salvetti cor- relation-energy formula into a functional of the electron density. Phys Rev B37:785–789

Michalska D (2003) RAINT program. Wroclaw University of Technology, Poland

Mishra A, Srivastava SK, Swati D, (2013) Study of structure–activity relationship of enantiomeric, protonated and deprotonated forms of warfarin via vibrational spectroscopy and DFT calculations. Spectrochim. Acta A: Mol. Biomol. Spectrosc.113: 439-446.

Moghanian H, Mobinikhaledi A, Monjezi R, (2013) Synthesis, spectroscopy (vibrational, NMR and UV–vis) studies, HOMO–LUMO and NBO analysis of 8-formyl-7-hydroxy-4-methylcoumarin by ab initio calculations. J. Mol. Struct. 1052: 135-145.

NIST Computational Chemistry Comparison and Benchmark Database, NIST Standard Reference Database Number 101, Release 12, 2005, Editor: Russell D. Johnson III, http://srdata.nist.gov/cccbdb.

Ramoji A, Yenagi J, Tonannavar J, Jadhav VB, Kulkarni MV, (2007) Vibrational assignments and electronic structure calculations for 3-acetylcoumarin. Spectrochim. Acta . 68: 504–509.

Sajan D, Erdogdu Y, Reshmy R, Dereli Ö, Thomas KK, Joe IH, (2011) DFT-based molecular modeling, NBO analysis and vibrational spectroscopic study of 3-(Bromoacetyl)coumarin. Spectrochim. Acta A: Mol. Biomol. Spectrosc 82: 118–125.

Sancheti S, Sancheti S, Seo SY (2013) Ameliorative effects of 7-methylcoumarin and 7-methoxycoumarin against CCl4-induced hepatotoxicity in rats. Drug Chem Toxicol. 36(1): 42-47.

Sarıkaya EK, Dereli Ö, (2014) Study on molecular structure and vibrational spectra of 5,7-dimethoxycoumarin using DFT: A combined experimental and quantum chemical approach. Optics and Spectroscopy. 117: 240-249.

Sarıkaya EK, Dereli Ö, (2013a) Molecular structure and vibrational spectra of 7-Ethoxycoumarin by density functional method. J Mol Struct. 1052: 214–220.

Sarıkaya EK, Dereli Ö, Erdogdu Y, Güllüoglu MT, (2013b) Molecular structure and vibrational spectra of 7-Ethoxycoumarin by density functional method. J Mol Struct. 1049: 220–226.

Shah A., Naliapara Y., Sureja D., Motohashi N., Kawase M., Miskolci C., Szabo D., Molnar J. (1998) 6,12-Dihydro-1-Benzopyrano[3,4-b][1,4]Benzothiazin-6-ones Synthesis and MDR Reversal in Tumor Cells. Anticancer Res. 18: 3001–3004.

Smith BC, (1998) Infrared Spectral Interpretation: A Systematic Aroach, CRC Press, Boca Raton, FL.

Spartan 08, Wavefunction Inc., Irvine, CA 92612, USA, 2008.

SQM version 1.0, Scaled Quantum Mechanical Force Field (2013) Green acres road. Fayetteville, Arkansas, p 72703

Sri NU, Chaitanya K, Prasad MVS, Veeraiah V, Veeraiah A, (2012) FT-IR, FT-Raman and UV–Vis spectra and DFT calculations of 3-cyano-4-methylcoumarin. Spectrochim. Acta A: Mol. Biomol. Spectrosc. 97: 728–736.

Subashchandrabose S, Krishnan A R, Saleem H, Thanikachalam V, Manikandan G, Erdogdu Y, (2010) FT-IR, FT-Raman, NMR spectral analysis and theoretical NBO, HOMO–LUMO analysis of bis(4-amino-5-mercapto-1,2,4-triazol-3-yl)ethane by ab initio HF and DFT methods J. Mol. Struc 981: 59-70.

Varsanyi G, (1973) Assignments for Vibrational Spectra of Seven Hundred Benzene Derivatives, s. 1–2, Academic Kiado, Budapest.

Yavari I, Djahaniani H, Nasiri F, (2006) The crystal structure of tert-butyl coumarin-3-carboxylate. J. Iran. Chem. Soc 3: 46-50.

Young D C, (2001) Computational Chemistry: A Practical Guide for Alying Techniques to Real World Problems, John Wiley & Sons, Canada.

Zolek T, Paradowska K, Wawer I, (2003) 13C CP MAS NMR and GIAO-CHF calculations of coumarins. Solid State Nucl. Magn. Reson. 23: 77–87.